REMARKS/ARGUMENT

Applicants submit herewith a copy of the reference listed in the IDS, "X.Li and J.A.Ritcey; Trellis Coded Modulation with Bit Interleaving and Iterative Decoding; IEEE Journal on Selected Areas in Communications, Vol. 17; Pages 715-724; 04/1999", as requested by the Examiner.

Claims 1-17 stand allowed.

Claims 18-20 stand rejected under 35 U.S.C. 103(a) as being unpatentable over Applicant Admitted Prior Art (AAPA) in view of Li et al. (Bit-Interleaved Coded Modulation with Iterative Decoding; IEEE Communications Letters; Nov. 1997 (pages 169-171). Applicants respectfully traverse this rejection, as set forth below.

Applicants respectfully point out that the Examiner has misconstrued prior art Figures 1 and 2 (the Applicant Admitted Prior Art (AAPA)) in the present application.

Figure 1 is identified as "a conventional wireless communication system which utilizes interleaving, turbo decoding and transmit diversity" (see page 5, lines 2-3). Reference numeral 11 refers to a transmitter (see page 7, line 4; page 9, lines 14-15). Reference numeral 12 refers to a separate receiver that receives the transmission from transmitter 12 (see page 7, lines 1-7). Thus transmitter 11 is a DUAL antenna transmitter having dual transmission paths. Transmitter 11 and receiver 12 are NOT part of the same device.

Figure 2 is identified as "a conventional wireless communication system that utilizes turbo coding, interleaving **and feed back of a posteriori probabilities from a SISO decoder**" (see page 5, lines 4-5). The transmitter in Figure 2 is a SINGLE antenna

transmitter having a single transmission path. Again, the transmitter and receiver in Figure 2 are NOT part of the same device.

The Examiner, however, identifies the AAPA transmitter as being: Fig. 1, a coder coupled to said input for performing a coding operation on said bit stream, said coder having an output for providing a result of said coding operation (Fig. 1, element 16); a first modulator coupled to said coder output for modulating said result, and a first antenna coupled to said first modulator for transmitting said modulated result on a wireless communication channel (Fig. 1, elements 11, & Specification, Page 2, lines 15-22); an interleaver coupled to said coder output for producing an interleaved version of said result (Fig. 2, element 21); and a second modulator coupled to said interleaver for modulating said interleaved version, and a second antenna coupled to said second modulator for transmitting said modulated interleaved version on a wireless communication channel (Fig. 1 & Fig. 2) (Office Action dated November 17, 2005, page 3, line 19 – page 4, line 4).

Applicants respectfully point out that the Examiner has improperly combined the dual antenna/dual transmission path transmitter of Figure 1 and the single antenna/single transmission path transmitter of Figure 2 without setting forth any justification for the combination (i.e., why one having ordinary skill in the art at the time of the invention would have been motivated to combine the transmitters of Figures 1 & 2) or discussing the ramifications of the changes that would have to be made in order to combine the two transmitters.

Similarly, the Examiner's determination that the transmitter of Figure 2 discloses a second modulator (Office Action dated November 17, 2005, page 4, lines 1-4) is simply erroneous. The single antenna/single transmission pathtransmitter of Figure 2 discloses only one modulator – NOT two.

The Examiner further relies upon Figure 2 for its teaching that interleaving is performed "after" encoding and going on to argue that there is no criticality in interleaving before the encoding or after the encoding process since it is a matter of design choice. Even if, arguendo, the Examiner determination were applicable to a single antenna/single transmission path transmitter, such as Figure 2, the transmitter of the present application is clearly a dual antenna/dual transmission path transmitter (see Fig. 3). As such, the Examiner's determination is not applicable.

When a dual antenna/dual transmission path transmitter is involved, however, placement of the interleaver(s) is more than just a matter of design choice. Figure 1 clearly shows the use of two coders (16 & 17) in the design case where the interleaver is coupled to an input of one of the decoders. In contrast, by coupling the interleaver 92 between the output of coder 91 and the input of modulator (mod.), **Applicants were able to omit one of the two coders, which results in a significant circuit/design savings to the present apparatus**. Nowhere does the Admitted Prior Art suggest such a savings in a dual antenna/dual transmission path transmitter. Moreover, the Examiner has failed to identify any other prior art that teaches or suggests such an implementation. As such, the Examiner has failed to present a prima facie case of the obviousness of Claim 18. The 35 U.S.C. 103(a) rejection of Claim 18 is overcome.

In proceedings before the Patent and Trademark Office, "the Examiner bears the burden of establishing a prima facie case of obviousness based upon the prior art". In re Fritch, 23 USPQ2d 1780, 1783 (Fed. Cir. 1992) (citing In re Piasecki, 745 F.2d 1468, 1471-72, 223 USPQ 785, 787-88 (Fed. Cir. 1984). "The Examiner can satisfy this burden only by showing some objective teaching in the prior art or that knowledge generally available to one of ordinary skill in the art would lead that individual to combine the relevant teachings of the references", In re Fritch, 23 USPQ2d 1780, 1783 (Fed. Cir. 1992)(citing In re Fine, 837 F.2d 1071, 1074, 5 USPQ2d 1596, 1598 (Fed. Cir. 1988)(citing In re Lalu, 747 F.2d 703, 705, 223 USPQ 1257, 1258 (Fed. Cir. 1988)).

Moreover, **the mere fact that the prior art may be modified in the manner suggested by the Examiner does not make the modification obvious unless the prior art suggested the desirability of the modification.** In re Gordon, 733 F.2d at 902, 221 USPQ at 1127. Moreover, **it is impermissible to use the claimed invention as an instruction manual or "template" to piece together the teachings of the prior art so that the claimed invention is rendered obvious.** In re Gorman, 933 F.2d 982, 987, 18 USPQ2d 1885, 1888 (Fed.Cir.1991). See also Interconnect Planning Corp. v. Feil, 774 F.2d 1132, 1138, 227 USPQ 543, 547 (Fed.Cir.1985). The Examiner has improperly "pieced together" the transmitters of Figures 1 and 2 without any evidence from the prior art suggesting such modification, as is required by law.

Furthermore, "all words in a claim must be considered in judging the patentability of that claim against the prior art." In re Wilson, 424 F.2d 1382, 1385, 165 USPQ 494, 496 (CCPA 1970). The Examiner has not considered all of the words of Claim 18 in judging the patentability of Claim 18 against the prior art.

Claims 19-20 stand allowable as depending (directly or indirectly) from allowable Claim 18 and by including further limitations not taught or suggested by the reference of record.
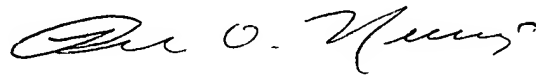
Claim 19 further defines the apparatus of claim 18, wherein said coder is a convolutional coder. Claim 19 depends from Claim 18 and is therefore allowable for the same reasons set forth above for the allowance of Claim 18.

Claim 20 further defines the apparatus of claim 18, wherein one of said first and second modulators is a QPSK modulator. Claim 20 depends from Claim 18 and is therefore allowable for the same reasons set forth above for the allowance of Claim 18.

Claim 21 is allowable for similar reasons to those set forth in support of the allowance of Claim 18.

Claims 1-17 stand allowed. Claims 18-21 stand allowable for the reasons presented above. Applicants respectfully request allowance of the application at the earliest possible date.

Respectfully submitted,

Ronald O. Neerings
Reg. No. 34,227
Attorney for Applicants

TEXAS INSTRUMENTS INCORPORATED
P.O. BOX 655474, M/S 3999
Dallas, Texas 75265
Phone: 972/917-5299
Fax: 972/917-4418

Trellis-Coded Modulation with Bit Interleaving and Iterative Decoding

Xiaodong Li, *Member, IEEE,* and James A. Ritcey, *Member, IEEE*

Abstract—This paper considers bit-interleaved coded modulation (BICM) for bandwidth-efficient transmission using software radios. A simple iterative decoding (ID) method with hard-decision feedback is suggested to achieve better performance. The paper shows that convolutional codes with good Hamming-distance property can provide both high diversity order and large free Euclidean distance for BICM–ID. The method offers a common framework for coded modulation over channels with a variety of fading statistics. In addition, BICM–ID allows an efficient combination of punctured convolutional codes and multiphase/level modulation, and therefore provides a simple mechanism for variable-rate transmission.

Index Terms—Bit interleaving, convolutional code, flat fading, iterative decoding, Rayleigh fading, signal labeling, trellis-coded modulation.

I. INTRODUCTION

THE programmable architecture of software radio promotes a flexible implementation of coding and modulation [1], [2]. This flexibility also translates into adaptivity, which can be used to optimize the throughput of a wireless data network, operating under varying channel conditions. The transmission rate can be adjusted by changing the code rate or the modulation constellation; either may require a new code, and therefore a new encoder/decoder (codec) in conventional trellis-coded modulation (TCM) approaches [3]. In addition, different channel fading statistics may lead to different design criteria, and therefore also different codecs [4]–[6]. Although it is theoretically possible to switch codecs frequently on a fully programmable architecture, a unified approach, without compromising performance, is highly desirable to simplify the implementation and real-time control. This even becomes necessary in a hybrid scheme where the decoder is implemented either with a special ASIC chip or with an FPGA device to alleviate the processing load.

This paper considers trellis-coded modulation using bit interleaving [7] and iterative decoding with hard decision feedback [8], [9]. The scheme not only achieves a performance gain over existing TCM schemes, but also provides a common framework for TCM over channels with a wide

X. Li was with the Department of Electrical Engineering, University of Washington, Seattle, WA 98195 USA. He is now with the Wireless Technology Research Department, Bell Laboratories, Lucent Technologies, Holmdel, NJ 07733 USA.

J. A. Ritcey is with the Department of Electrical Engineering, University of Washington, Seattle, WA 98195 USA.

variety of fading statistics. In addition, the system allows an efficient combination of punctured convolutional codes and multiphase/level modulation, and therefore offers a simple mechanism for variable-rate transmission [10]. The paper begins with a short description of the relevant TCM literature, to emphasize the foundations of the suggested scheme.

TCM was first proposed by Ungerboeck [3] to efficiently combine convolutional coding and multiphase/level modulation. Through signal set expansion, TCM achieves large coding gain without reducing bandwidth efficiency. In a famous example by Ungerboeck [11], TCM with a four-state, rate-2/3 code, and 8PSK modulation performs 3 dB better than uncoded QPSK, while maintaining the same spectral efficiency. The key features of TCM include signal set expansion, set partitioning (SP) labeling, and joint code and modulation design.

For additive white Gaussian noise (AWGN) channels, the design criterion for TCM is to maximize the free Euclidean distance between coded signals. However, when TCM is designed for fully interleaved Rayleigh fading channels, that emphasis shifts to providing a large diversity order, with a secondary goal of large product distance [4]–[6]. A good example is the bit-interleaved coded modulation (BICM) method first suggested by Zehavi [7], [12]–[14].

Conventional interleaving for fading channels is symbol based, so the diversity order is the smallest number of different channel *symbols* between any two possible coded sequences. With a bit interleaver, the diversity order can be further increased to the binary Hamming distance of a code [7]. Convolutional codes with the best free Hamming distances [15] are optimal. The increased diversity steepens the bit error rate (BER) curve, significantly improving TCM for Rayleigh fading. In addition, BICM treats coding and modulation as two separate entities. From a practical point of view, this allows more flexibility in design and implementation, compared with the joint code/modulation approach by TCM.

A known pitfall of BICM is the reduced free Euclidean distance caused by the "random modulation" inherent in a bit-interleaved scheme [7], [6]. This results in performance degradation over conventional TCM for AWGN channels. Likewise, when the fading is slow and the interleaving insufficient, conventional TCM can outperform BICM.

In [8] and [9], the authors show that the performance of BICM can be improved by iterative decoding (ID) using hard-decision feedback. In particular, BICM–ID converts a 2^M-ary signaling channel to M parallel binary channels. With proper bit labeling, a large binary Hamming distance between coded bits can be indirectly translated into a large Euclidean distance.
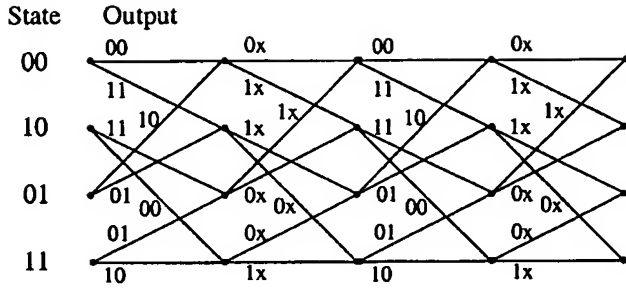
Fig. 1.   Trellis diagram of a rate-2/3, four-state punctured code obtained from its rate-1/2 mother code. "x" represents a punctured bit.

TABLE I
PUNCTURE PATTERNS FOR THE 16-STATE RCPC CODES [17]

Code Rate (R)	Puncture Pattern	d_H
1/2	1111 1111	7
2/3	1111 1x1x	4
4/5	1111 1xxx	3

This simultaneously realizes high diversity order *and* large free Euclidean distance, and effectively combines powerful binary codes with bandwidth-efficient modulation. Simulation results show that BICM–ID improves BICM by more than 1 dB for both channel types. With this improvement, BICM–ID compares favorably with TCM over AWGN channels, while significantly outperforming the latter over fading channels.

Punctured convolutional codes were first suggested by Cain *et al.* [16] to reduce the decoding complexity of high-rate codes. With punctured codes, the information bits are first coded with a low-rate code, e.g., rate-1/2. Only a subset of the coded bits is transmitted—others are removed according to a puncture pattern, as shown in Fig. 1 and Table I. This leads to a higher code rate. Also, a family of codes with different rates, all punctured from the same mother code, share a single encoder/decoder. The concept of punctured codes was extended to rate-compatible punctured convolutional (RCPC) codes by Hagenauer [17]. With RCPC codes, all of the transmitted coded bits are a subset of a lower rate code. This permits an increase in the code redundancy by incremental transmission, and can be combined with ARQ schemes to improve the efficiency of data communications.

Using punctured codes for TCM simplifies the implementation, but often leads to a performance degradation compared with Ungerboeck codes. Many methods have been suggested to overcome this problem [18]–[20]. However, most of the approaches are optimized for only a specific code rate or a certain channel type. In this paper, BICM–ID design is combined with RCPC codes [10]. It achieves good performance for various channel conditions, and allows a simple implementation of variable-rate transmission.

The paper is organized as follows. Section II introduces BICM–ID, including the key calculation of the bit metrics and labeling of the signal constellation. It also addresses some of the implementation issues related to software ra-

dios. Section III evaluates performance and shows simulation results. Section IV concludes the paper.

II. BIT-INTERLEAVED CODED MODULATION WITH ITERATIVE DECODING (BICM–ID)

A. System Description

Fig. 2 shows the block diagram of BICM–ID. Due to the weak coupling between the code and modulation in BICM–ID, a variety of binary convolutional codes and modulation methods can be flexibly combined. Also, convolutional codes punctured from a single mother code can be used to enhance flexibility. For simplicity, the discussion below focuses on a rate-2/3 code and 8PSK modulation.

Input information bits are first encoded by a convolutional encoder. Then, a bit-by-bit interleaver permutes the order of encoder output bits. Note that the interleaver is composed of three independent bit interleavers corresponding to the three bit positions in an 8PSK symbol. The interleaved bits are grouped into modulation symbols. The purpose of bit-by-bit interleaving is, first, to break the correlation of sequential fading coefficients, and to maximize the diversity order of the system [7]. Second, it removes the correlation among the sequentially coded bits, as well as the bits associated with the same channel symbol. This is important in reducing error propagation in the iterative decoding.

Denoting an interleaver output 3-tuple by $V_t = [v_t^1, v_t^2, v_t^3]$, a signal labeling map by μ, and the corresponding 8PSK signal at time t by x_t,

$$x_t = \mu(V_t), \qquad x_t \in \chi \qquad (1)$$

where the 8PSK signal set is $\chi = \{\sqrt{E_s}\,e^{j2n\pi/8}, \ n = 0, \cdots, 7\}$ and E_s is the energy per channel symbol. With a rate-2/3 convolutional code, the energy per information bit is $E_b = E_s/2$. For a flat Rayleigh fading channel with coherent detection, the received discrete-time signal is

$$y_t = \rho_t x_t + n_t \qquad (2)$$

where ρ_t is the Rayleigh-distributed fading amplitude with $E(\rho_t^2) = 1$ and n_t is complex AWGN with variance $\sigma_I^2 = \sigma_Q^2 = N_0/2$. For an AWGN channel, $\rho_t = 1$. It is assumed throughout the paper that the channel state information (CSI) ρ_t is accurately estimated at the decoder either through pilot symbols or pilot tones. The degradation caused by the lack of CSI is small for 8PSK [21], while CSI is essential for 16QAM.

B. Conventional Maximum Likelihood Bit-Metric Calculation

With conventional decoding for BICM [7], [12]–[14], the log-likelihood bit metrics λ are calculated for the two possible binary values b of each coded bit v_t^i at time t according to

$$\begin{aligned}
\lambda(v_t^i = b) &= \log \sum_{x \in \chi(i,\,b)} P(y_t|x, \rho_t) \\
&\approx \max_{x \in \chi(i,\,b)} \log P(y_t|x, \rho_t) \\
&\sim \min_{x \in \chi(i,\,b)} \|y_t - \rho_t x\|^2, \qquad i = 1, 2, 3; \ b = 0, 1
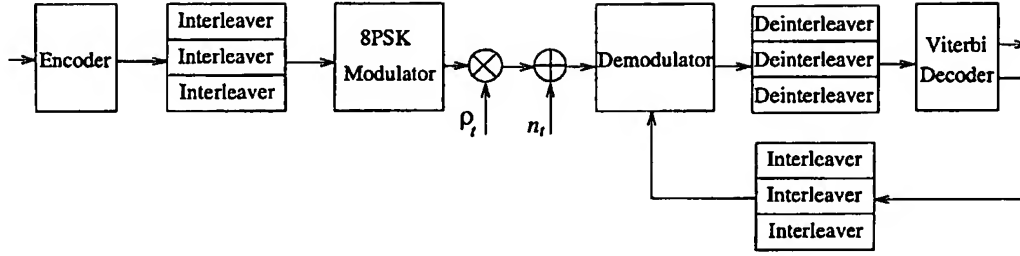\end{aligned}$$

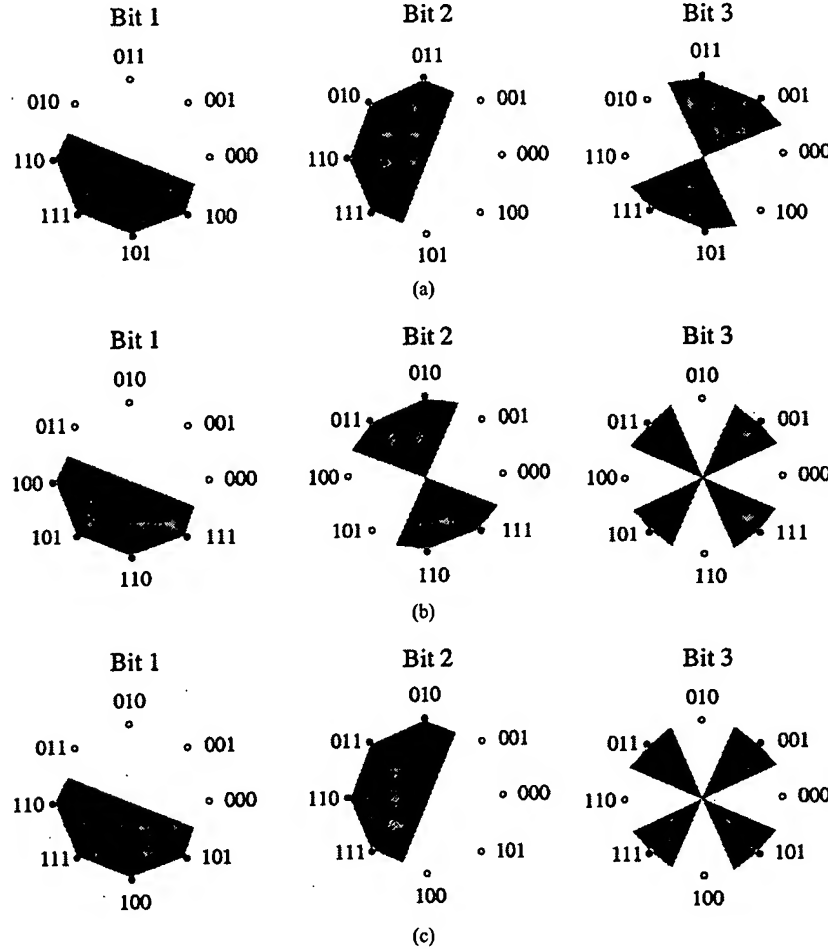$$(3)$$

Fig. 2. Block diagram of BICM–ID.

Fig. 3. Three labeling methods for 8PSK and their corresponding subset partitioning for each bit. (a) Gray, (b) self-partitioned, and (c) mixed labeling.

where the signal subsets are $\chi(i, b) = \{\mu([v^1, v^2, v^3])|v^i = b\}$ and the approximation is good at high signal-to-noise ratio (SNR) [7]. Examples of the subsets are the shaded symbols in Fig. 3, which will be discussed in more detail later. Six bit metrics (three bit positions, each with binary values 0 and 1) are generated from each received channel symbol. As shown in Fig. 4, the bit metric for the first bit with a value of 1 is

$$\lambda(v_t^1 = 1) = \min(d_{100}^2, d_{101}^2, d_{110}^2, d_{111}^2) \qquad (4)$$

and the bit metric for the first bit with a value of 0 is

$$\lambda(v_t^1 = 0) = \min(d_{000}^2, d_{001}^2, d_{010}^2, d_{011}^2) \qquad (5)$$

where d_i^2 ($i = 000, \cdots, 111$) is the squared Euclidean distance between the received signal y_t and the faded version of the transmitted signal i. For 8PSK, the distance can be simplified using the signal correlation. The bit metrics for the other two bit positions $\lambda(v_t^2 = 1)$, $\lambda(v_t^2 = 0)$, $\lambda(v_t^3 = 1)$, and $\lambda(v_t^3 = 0)$ are generated in a similar way.

The trellis branch metrics are formed by summing the corresponding deinterleaved bit metrics. Finally, the standard Viterbi algorithm is used at decoding. Since BICM is bit oriented, the decoding for punctured codes is straightforward—if a bit is punctured at the encoder, the associated bit metrics are taken as zero at the decoder.
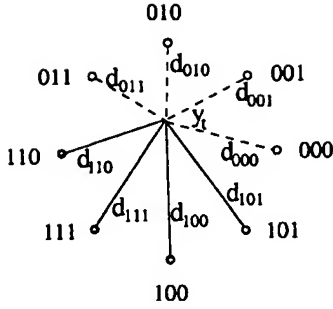
Fig. 4. Bit metric calculation for BICM.

C. Iterative Decoding with Hard-Decision Feedback

The metric (3) is a simplification of the *a posteriori* probabilities

$$P(v_t^i = b | y_t) = \sum_{x \in \chi(i, b)} P(x | y_t, \rho_t)$$

$$\sim \sum_{x \in \chi(i, b)} P(y_t | x, \rho_t) P(x),$$

$$i = 1, 2, 3; \; b = 0, 1 \quad (6)$$

where $P(x)$ are the *a priori* probabilities and the terms common to all i and b are disregarded. This simplification, while reducing complexity, can lead to performance loss for two reasons. First, convolutional encoding introduces redundancy and memory into the coded signal sequence. Yet, the assumption of equal likelihood on $P(x)$ in (3) fails to use this information, primarily because it is difficult to specify $P(x)$ in advance of *any* decoding. Second, the individual minimization operations for the bit metrics may lead to self-contradictory assumptions on the values of the bits making up a channel symbol.

To improve (3), note that the *a priori* information is reflected in the decoding results, and therefore can be included through iterative decoding. Note further that the concept of iterative decoding, or iterative processing in general, is not new. Its most recent success is in "turbo codes" [22]. Also, iterative decoding has been considered for multilevel codes [23], [24].

To find $P(x)$, one might use a symbol-by-symbol *a posteriori probability* algorithm [25], [26] or a Viterbi decoder with soft output [27]. There is a low-complexity alternative, however. Retain the conventional Viterbi decoder, and consider only binary hard-decision feedback in the calculation of the bit metrics on the second pass of decoding. This also avoids the self-contradictory assumptions mentioned earlier. For example, to calculate $\lambda(v_t^1 = 1)$, assume, for any $x = \mu(v^1, v^2, v^3) \in \chi(1, 1)$

$$P(x) = \begin{cases} 1, & \text{if } v^1 = 1, v^2 = \hat{v}_t^2, v^3 = \hat{v}_t^3 \\ 0, & \text{otherwise} \end{cases} \quad (7)$$

where $\hat{v}_t^2$ and $\hat{v}_t^3$ are the first-pass decoding decisions. Then the bit metric with the decision feedback becomes

$$\lambda'(v_t^1 = 1) = \left\| y_t - \rho_t \mu([1, \hat{v}_t^2, \hat{v}_t^3]) \right\|^2. \quad (8)$$

That is, take the results of the earlier pass of decoding as correct. For example, suppose that the first-pass decoding

decisions for the second and third coded bit are $\hat{v}_2 = 0, \hat{v}_3 = 1$, the bit metric for $v_t^1 = 1$ for the second-pass decoding is simply

$$\lambda'(v_t^1 = 1) = d_{101}^2. \quad (9)$$

The newly generated bit metrics are used in Viterbi decoding again, and the process continues iteratively.

To avoid severe error propagation, the feedback bits should be independent of the bit for which the bit metric is calculated. This is made possible by the three bit interleavers. The three bits making up a channel symbol are typically far apart in the coded sequence. Further enhancement can be achieved by the joint optimization of the interleavers to assure bit independence [26].

D. Signal Labeling

Signal labeling is a critical part of BICM–ID. The effects of different labeling methods are presented graphically in Figs. 3 and 5.

Fig. 3 illustrates the subset partitioning for each of the three bit positions for three different labeling methods: Gray labeling, SP labeling, and mixed labeling. The graphical representation was first used by Zehavi for BICM with Gray labeling in [7]. The shaded regions (only shown inside the unit circle) correspond to $\chi(i, 1)$, and the unshaded to $\chi(i, 0)$ ($i = 1, 2, 3$). These are also the decision regions for each bit if hard-decision detection were made for each bit *individually* before convolutional decoding. It is clear that the three labeling methods have the same intersubset Euclidean distances, but different numbers of nearest neighbors, or different Hamming-distance properties of the labels for neighboring constellation points. For the first-pass decoding performance, Gray labeling apparently suits the best, and is extensively used for BICM [7], [12], [14].

At the second-pass decoding, given the feedback of bits 2 and 3, the constellation of bit 1 is confined to a pair of points as shown in Fig. 5. Therefore, as far as bit 1 is concerned, *the 8PSK channel is translated into a binary channel, with a BPSK constellation selected (by the two feedback bits) from the four possible signal pairs*. The same is true for bits 2 and 3. To optimize the second-pass decoding performance, one must maximize the Euclidean distance between the two points of all pairs. Among the three methods, SP labeling best serves this purpose, while Gray labeling is the worst.

Of course, feedback errors lead to wrong selections of signal pairs. Therefore, the overall decoding performance also depends on the first-pass performance and the robustness of a labeling method to the feedback errors. A compromise between optimizing the first-pass decoding performance and maximizing the improvement provided by iterative decoding leads to the mixed labeling method, which is confirmed by computer simulation to outperform both Gray labeling and SP labeling for AWGN as well as Rayleigh channels. Note that mixed labeling, named so as to emphasize the compromise between Gray and SP labeling, is used by others [19], [28]. In [28], it is called "reordered" mapping. Also note that mixed labeling optimizes the performance of BICM–ID with
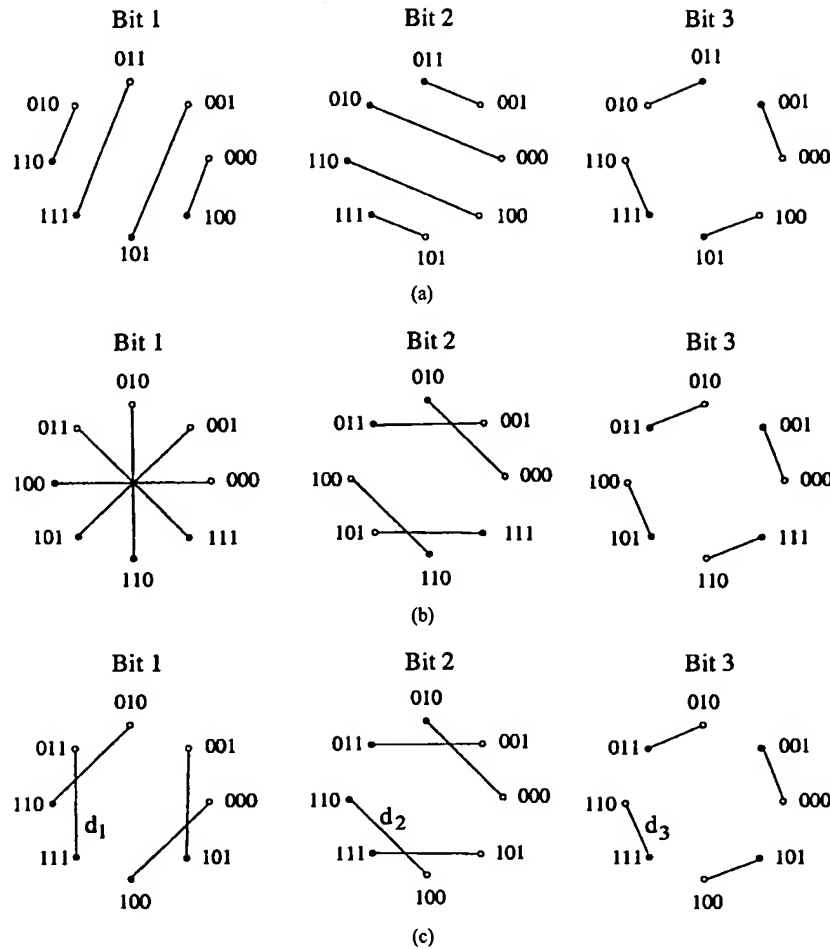
Fig. 5. Iterative decoding with hard-decision feedback translates the 8PSK channel into three parallel binary channels, each with a BPSK constellation selected (by the other two feedback bits) from the four possible signal pairs. (a) Gray labeling, (b) set partitioning labeling, and (c) mixed labeling.

hard-decision feedback. As shown in [26], when a more sophisticated soft-feedback method is used to minimize the error propagation, SP labeling actually performs the best.

E. Complexity Issues

This section addresses the implementation issues. To better focus on the topics covered in this paper, it considers only the function modules of the encoder/decoder and digital modulator/demodulator. The complexity differences among TCM, BICM, and BICM–ID are also emphasized.

The implementation of convolutional encoding is simple. Usually, a lookup table describing one section of trellis is stored in the on-chip memory. The encoder finds the next state and the output according to the input and the trellis transition table. Digital modulation can also be implemented with table lookup. The computation and memory requirements for these two parts are usually very low and insignificant compared with other modules. For encoding and modulation, the three coded-modulation schemes compared here have roughly the same complexity.

The digital demodulator provides the appropriate metrics for soft-decision Viterbi decoding. For each received complex signal, BICM first calculates the channel symbol metrics, the

distance values as shown in (3). For TCM, the symbol metrics are the same as the branch metrics for the Viterbi decoder. However, for BICM, bit metrics need to be generated from the symbol metrics, and then regrouped to form the branch metrics for decoding. For BICM–ID, the demodulation on the first pass is the same as BICM. But additional operations are required for the bit-metric regeneration. Note that all of the symbol metrics used in (8) have been calculated during the first pass. On the following passes, only reselections of the previously computed data are needed.

Interleaving or deinterleaving usually requires few CPU cycles, but demands a large amount of memory access. So, the execution time strongly depends on the chip architecture as well as the length and structure of the interleaver. To speed up the process, especially for large interleavers, smart DMA modes such as background data movement (data ping-ponging) and programmable data packet transfer are desirable.

For convolutionally coded modulation, the major computational load is in the Viterbi decoding. Its complexity is measured as follows. Suppose that the number of trellis states is $S = 2^\nu$, where ν is the code memory. The number of branches entering or leaving each state is $B = 2^k$, where k is the number of input information bits per stage. Each state

at each trellis stage requires B additions for metric updating, $B - 1$ comparisons, and one selection. So the total number of operations per information bit is proportional to

$$T = 2BS/k = 2^{(k+\nu+1)}/k. \tag{10}$$

The complexity increases exponentially with the code memory. In addition, (10) shows the advantage of implementing a high-rate code (large k) using the punctured code obtained from a mother code with $k = 1$. Of course, (10) is only a rough approximation. The number of CPU cycles for different operations will depend heavily on the software implementation and on the processor architecture. Furthermore, the overhead of memory access may significantly effect the execution speed.

Note that, by purely counting the number of operations, decoding twice or doubling the number of code states leads to roughly the same increase in computation. However, the latter requires twice the on-chip memory to store accumulated metrics and survivor paths. Note that, due to the use of interleaving, all of the received signals or their associated metrics in a block need to be stored. But these data do not have to be all on chip at the same time. If the decoder is implemented using an ASIC, then decoding twice requires twice the clock cycles, but increases the hardware complexity only a little.

A large block size is often desirable for iterative decoding, including BICM–ID. The simulations use 2000 information bits for each block, comparable to the length of a 255-symbol Reed–Solomon code, often considered for wireless data networking [29]. The implications of such a block length on the buffer size and transmission latency need to be carefully considered. The block length for BICM–ID can be significantly reduced with little effect on the fading-channel performance, but can cause degradation over AWGN channels. For PCS applications with fixed data rate, relaxed BER requirement, and very low tolerance for latency, BICM without iterative decoding is an attractive approach.

III. PERFORMANCE EVALUATION

A. Performance Analysis Assuming Error-Free Feedback

A closed-form performance evaluation of BICM–ID is difficult, partly because of the nonlinear iterative processing. An evaluation of the idealized situation assuming error-free feedback (EFF) provides insight into BICM–ID. A justification of this approach can be found in a follow-up paper [26], which shows that the performance of BICM–ID using soft feedback converges to the EFF performance, and the degradation of hard-decision feedback over soft-decision feedback is small *when mixed labeling is used*. The actual performance of BICM–ID is found by computer simulation.

1) AWGN Channels: Consider the pairwise error probability $P(\hat{C}|C)$, the probability that a code sequence C is transmitted, but a code sequence $\hat{C}$ is selected at the decoder. Denote w_i ($i = 1, 2, 3$) as the Hamming distances between $\hat{C}$ and C corresponding to the ith bit position in an 8PSK symbol. BICM–ID with EFF translates the 8PSK channel into three independent BPSK channels with intersignal Euclidean

TABLE II
SQUARED FREE EUCLIDEAN DISTANCES OF TCM, BICM, AND BICM–ID (ASSUMING EFF); RATE-2/3 CODES AND 8PSK MODULATION WITH $E_s = 1$; RCPC CODES FOR BICM AND BICM–ID

# of States	TCM	BICM	BICM-ID
8	4.59	2.34	5.17
16	5.17	2.34	6.34
32	5.76	3.51	7.75
64	6.34	3.51	8.34

distances d_1, d_2, and d_3 shown in Fig. 5(c). The squared Euclidean distance between the two modulated sequences is $d^2(\hat{C}, C) = w_1 d_1^2 + w_2 d_2^2 + w_3 d_3^2$, and the pairwise error probability is

$$P(\hat{C}|C) = Q\left(\sqrt{\frac{d^2(\hat{C}, C)}{2N_0}}\right) \tag{11}$$

where $Q(x) = \int_x^\infty e^{-t^2/2}\, dt/\sqrt{2\pi}$ is the error function.

The squared free Euclidean distance d_E^2 of BICM–ID conditioned on EFF depends on the weight distribution w_i ($i = 1, 2, 3$) of the corresponding error event. On the other hand, it can be shown that for BICM with conventional decoding, $d_E^2 \le d_H\, d_3^2$, where d_H is the free Hamming distance of the code and d_3, as shown in Fig. 5(c), is the minimum Euclidean distance between constellation points. The equivalence is achieved with Gray labeling. Since d_1 and d_2 are significantly larger than d_3 for mixed labeling, BICM–ID assuming EFF can provide larger d_E^2 than BICM.

Table II lists d_E^2 for TCM, BICM, and BICM–ID with rate-2/3 codes and 8PSK modulation. BICM and BICM–ID use RCPC codes [17] to facilitate the practical implementation, although slightly better performance can be obtained with optimal, nonpunctured codes [15]. As explained before, BICM uses Gray labeling, while BICM–ID uses mixed labeling. Table II shows that d_E^2 of BICM is smaller than that of TCM. This explains the performance degradation of BICM over AWGN channels. However, BICM–ID assuming EFF provides better d_E^2 than TCM. Therefore, it is *possible* that BICM–ID, with actual feedback, can outperform TCM.

2) Rayleigh Fading Channels: Following [7], a Chernoff bound for the pairwise error probability for Rayleigh fading channels can be found:

$$P(\hat{C}|C) \le \left(\cfrac{1}{1 + \cfrac{d_1^2}{4N_0}}\right)^{w_1 + w_2} \left(\cfrac{1}{1 + \cfrac{d_3^2}{4N_0}}\right)^{w_3} \tag{12}$$

where mixed labeling is assumed and $d_1 = d_2$. Note that the time diversity $d_H = w_1 + w_2 + w_3$, the same as BICM. Comparing (12) and [7, e.g. (4.6)], one may notice that BICM–ID improves the product distance. The diversity orders of symbol-interleaved TCM and BICM/BICM–ID for rate-2/3 codes with various memories are listed in Table III.

B. Simulation Results

Consider the performance of BICM–ID with 8PSK modulation for AWGN and Rayleigh fading channels. RCPC codes
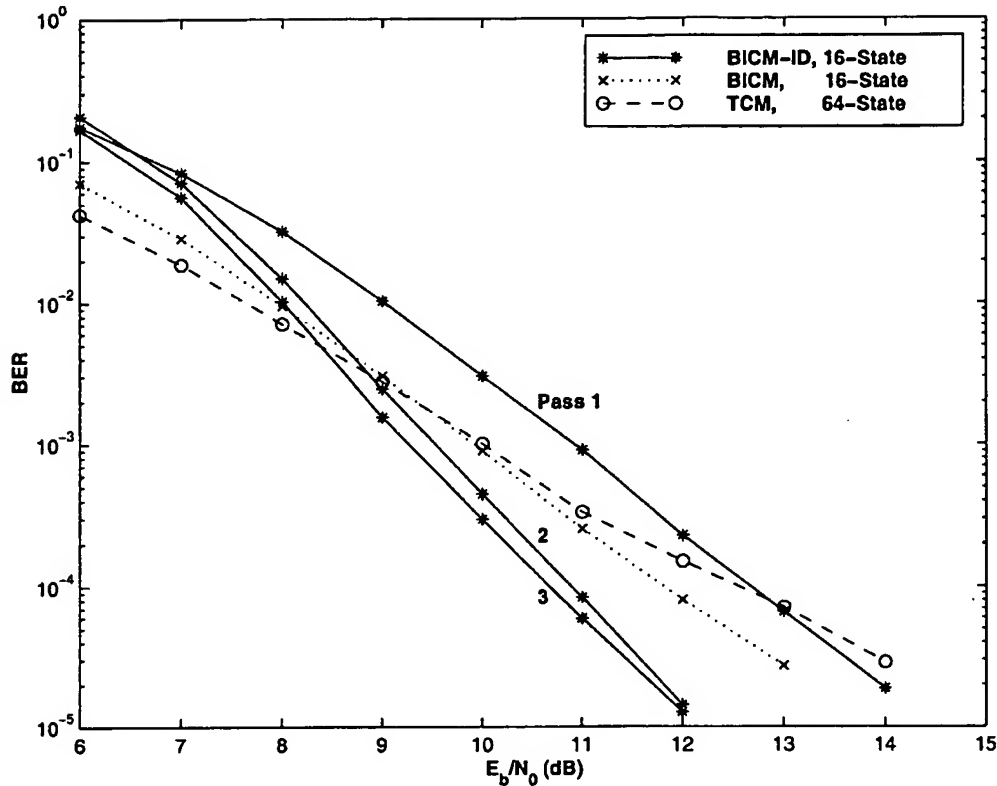
Fig. 6. Performance of BICM–ID with the rate-2/3 RCPC code and 8PSK modulation over Rayleigh fading channels.

TABLE III
TIME DIVERSITIES OF TCM AND BICM/BICM–ID WITH
RATE-2/3 CODES; RCPC CODES FOR BICM AND BICM–ID

# of States	TCM	BICM/BICM-ID
8	2	4
16	3	4
32	2	6
64	3	6

obtained from the rate-1/2, 16-state mother code are used to achieve various code rates [17]. The puncturing patterns and the corresponding free Hamming distances are listed in Table I. The simulation of Ungerboeck's TCM and BICM without iterative decoding is included for comparison. Gray labeling is used for BICM, while mixed labeling is used for BICM–ID. Each data block contains 2000 information bits. For each BER data point, 10^7 information bits are simulated.

Fig. 6 shows the performance of BICM and BICM–ID with the rate-2/3 code over Rayleigh channels. BICM with the 16-state code and a time diversity of 4 outperforms the 64-state TCM with a time diversity of 3. Due to its use of mixed labeling instead of Gray labeling, BICM–ID performs about 1 dB worse than BICM on the first pass of decoding. However, with a second pass, BICM–ID quickly catches up and outperforms BICM by more than 1 dB. A third pass of decoding adds slight improvement. BICM–ID with two decoding passes outperforms the 64-state TCM by more than 2 dB.

The performance for AWGN channels is shown in Fig. 7. There is only a small difference between TCM and BICM–ID

with three decoding passes. Adding another decoding pass, BICM–ID matches the performance of 64-state TCM. The gain of BICM–ID over BICM is about 2 dB. Note that the sharp slope of the BER curves of BICM–ID is characteristic for iterative decoding. After converging with the EFF bound at high SNR, the BER curves of BICM–ID are flatter [26].

Figs. 8 and 9 show the performance of BICM–ID using RCPC codes with various code rates over Rayleigh and AWGN channels. By varying the throughput, reliable communications can be achieved for a wide range of channel conditions. Note that the improvement through iterative decoding is more significant for low code rates. This is useful for battling against highly degraded channels. Further adaptivity can be achieved by varying the modulation scheme.

Note that each data block contains 2000 information bits in the simulation. A shorter block length may cause degradation over AWGN channels, but has little effect on the performance over Rayleigh channels. For example, other simulations show that BICM–ID with a block of 500 information bits has about 1 dB degradation on the fourth pass at BER = 10^{-5}, compared with the results shown in Fig. 7 for AWGN channels, but gives almost the same performance as shown in Fig. 6 for fading channels. Also note that all of the curves shown in the figures are the averaged error rates of *information bits* (encoder input), not for those of *coded bits* (encoder output). In fact, as in BICM or in multilevel coding schemes, the individual BER for each coded bit position may be different due to different mappings shown in Fig. 3. For example, the BER performance of bit 3 is about 0.5 dB inferior to that of bits
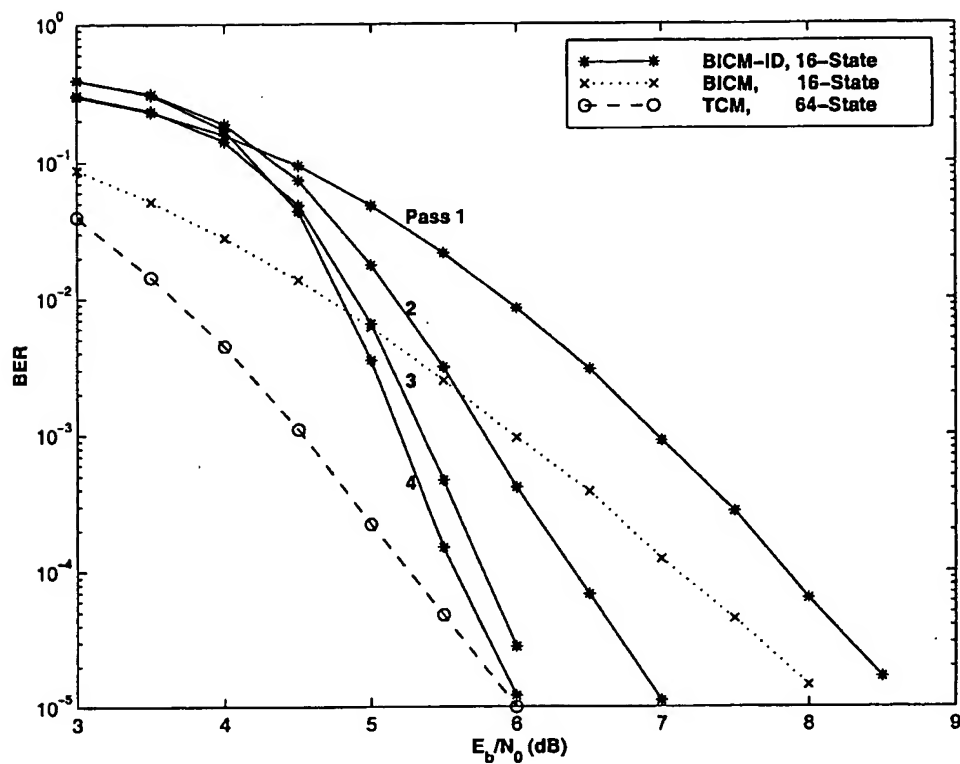
Fig. 7.   Performance of BICM–ID with the rate-2/3 RCPC code and 8PSK modulation over AWGN channels.
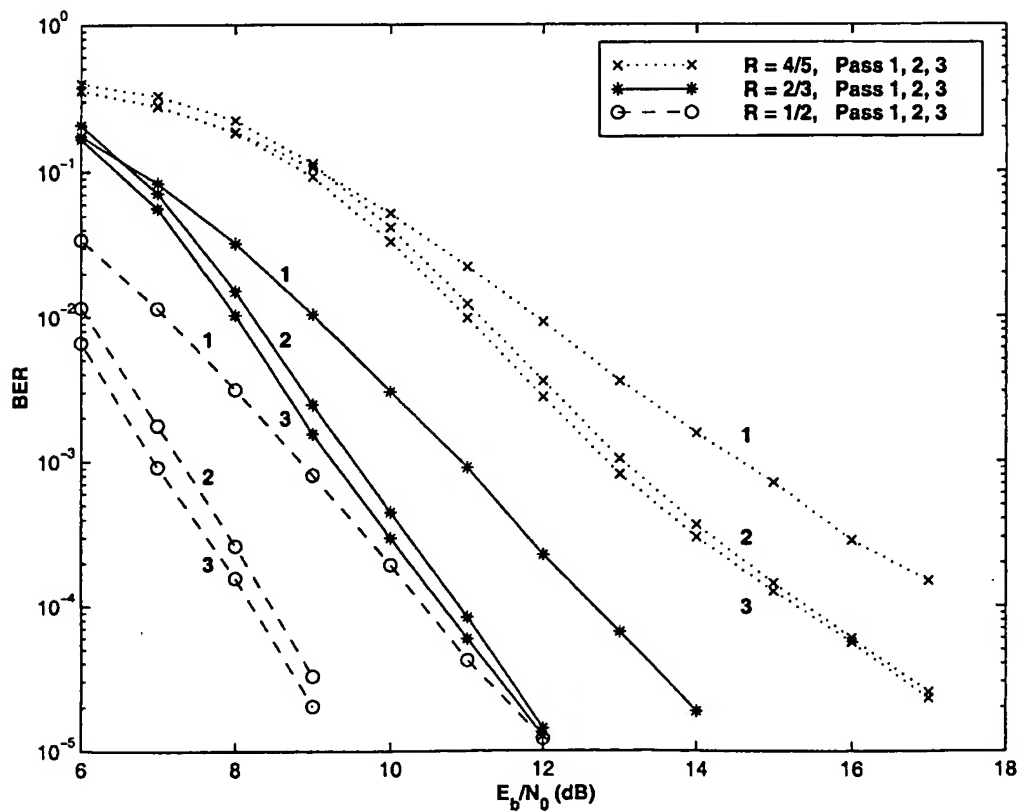

Fig. 8.   Performance of BICM–ID using RCPC codes with various code rates and 8PSK modulation over Rayleigh fading channels.
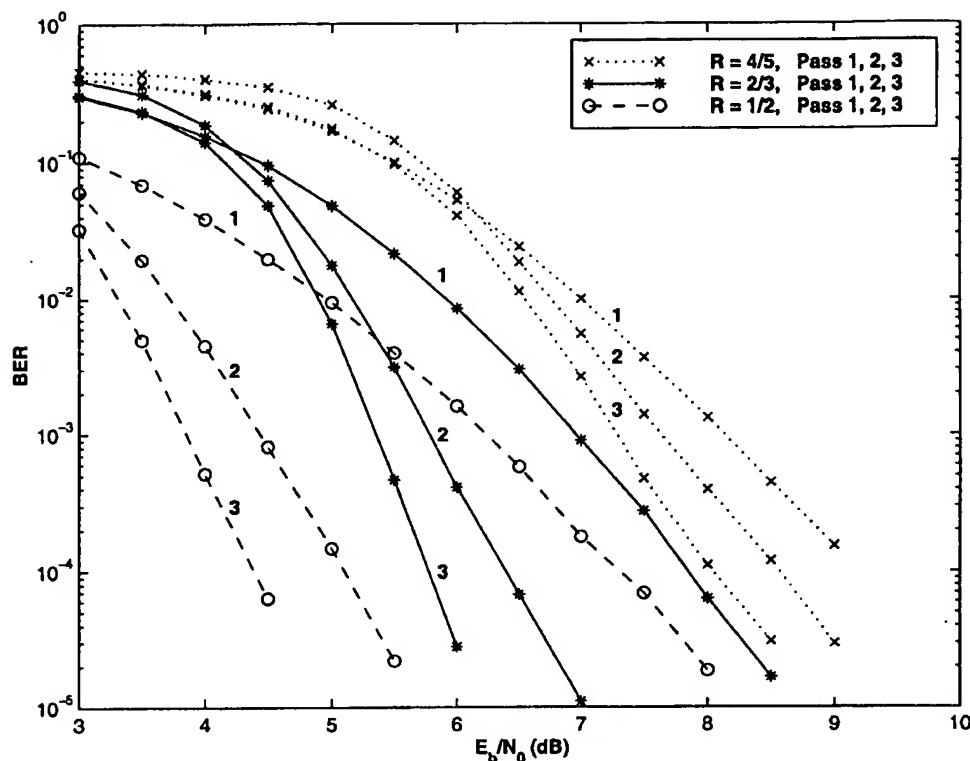
Fig. 9. Performance of BICM–ID using RCPC codes with various code rates and 8PSK modulation over AWGN channels.

1 and 2 in BICM–ID. However, unlike those in multilevel coding schemes [23], [24], the two information bit positions have virtually the same BER performance.

IV. CONCLUSIONS

BICM–ID outperforms conventional TCM over Rayleigh fading channels, and compares favorably with TCM over AWGN channels. Through the use of punctured codes, BICM–ID provides a simple mechanism for variable-rate transmission. Its features, attractive in software radios, are also suitable for hybrid approaches using ASIC's or FPGA's.

REFERENCES

[1] J. Mitola, "The software radio architecture," *IEEE Commun. Mag.*, vol. 33, pp. 26–45, May 1995.

[2] Z. Kostic and S. Seetharaman, "Digital signal processors in cellular radio communications," *IEEE Commun. Mag.*, vol. 35, pp. 22–35, Dec. 1997.

[3] G. Ungerboeck, "Channel coding with multilevel/phase signals," *IEEE Trans. Inform. Theory*, vol. IT-28, pp. 56–67, Jan. 1982.

[4] D. Divsalar and M. K. Simon, "The design of trellis coded modulation for MPSK for fading channels: Performance criteria," *IEEE Trans. Commun.*, vol. 36, pp. 1004–1012, Sept. 1988.

[5] C. Schlegel and D. Costello, "Bandwidth efficient coding for fading channels: Code construction and performance analysis," *IEEE J. Select. Areas Commun.*, vol. 7, pp. 1356–1368, Dec. 1989.

[6] C.-E. W. Sundberg and N. Seshadri, "Coded modulation for fading channels: An overview," *Eur. Trans. Telecommun.*, vol. 4, pp. 325–334, May–June 1993.

[7] E. Zehavi, "8-PSK trellis codes for a Rayleigh fading channel," *IEEE Trans. Commun.*, vol. 40, pp. 873–883, May 1992.

[8] X. Li and J. A. Ritcey, "Bit-interleaved coded modulation with iterative decoding," *IEEE Commun. Lett.*, vol. 1, pp. 169–171, Nov. 1997.

[9] _____, "Low-complexity MAP decoding of trellis coded modulation with bit interleaving," in *Proc. IEEE GLOBECOM'97, Commun. Theory Mini-Conf.*, Nov. 1997, pp. 28–32.

[10] _____, "Variable-rate trellis coded modulation using punctured codes," in *Proc. PACRIM'97*, Aug. 1997, pp. 624–627.

[11] G. Ungerboeck, "Trellis-coded modulation with redundant signal sets, Part I: Introduction," *IEEE Commun. Mag.*, vol. 25, pp. 5–11, Feb. 1987.

[12] U. Hansson and T. Aulin, "Channel symbol expansion diversity-improved coded modulation for the Rayleigh fading channels," in *Proc. IEEE ICC'96*, June 1996, pp. 891–895.

[13] S. A. Al-Semari and T. E. Fuja, "Bit interleaved I-Q TCM," in *Proc. ISITA'96*, Sept. 1996, pp. 16–19.

[14] G. Caire, G. Taricco, and E. Biglieri, "Bit-interleaved coded modulation," in *Proc. IEEE ICC'97*, June 1997, pp. 1463–1467.

[15] S. Lin and D. J. Costello, Jr., *Error Control Coding: Fundamentals and Applications.* Englewood Cliffs, NJ: Prentice Hall, 1983.

[16] J. B. Cain, G. C. Clark, and J. M. Geist, "Punctured convolutional codes of rate $(n-1)/n$ and simplified maximum likelihood decoding," *IEEE Trans. Inform. Theory*, vol. IT-25, pp. 97–100, Jan. 1974.

[17] J. Hagenauer, "Rate-compatible punctured convolutional codes (RCPC codes) and their applications," *IEEE Trans. Commun.*, vol. 36, pp. 389–400, Apr. 1988.

[18] J. K. Wolf and E. Zehavi, "P^2 codes: Pragmatic trellis codes utilizing punctured convolutional codes," *IEEE Commun. Mag.*, vol. 33, pp. 94–99, Feb. 1995.

[19] J. Kim and G. J. Pottie, "On punctured trellis coded modulation," *IEEE Trans. Inform. Theory*, vol. 42, pp. 627–636, Mar. 1996.

[20] F. Chan and D. Haccoun, "Performance of punctured trellis coded modulation over fading channels," in *Proc. IEEE VTC'97*, May 1997, pp. 339–343.

[21] S. G. Wilson and Y. S. Leung, "Trellis-coded phase modulation on Rayleigh channels," in *Proc. IEEE ICC'87*, June 1987, pp. 739–743.

[22] C. Berrou, A. Glavieux, and P. Thitimajshima, "Near Shannon limit error-correcting coding and decoding: Turbo-codes (1)," in *Proc. IEEE ICC'93*, May 1993, pp. 1064–1070.

[23] T. Woerz and J. Hagenauer, "Iterative decoding for multilevel codes using reliability information," in *Proc. IEEE GLOBECOM'92*, Dec. 1992, pp. 1779–1784.

[24] N. Seshadri and C.-E. W. Sundberg, "Multilevel trellis coded modulations for the Rayleigh fading channel," *IEEE Trans. Commun.*, vol. 41, pp. 1300–1310, Sept. 1993.

[25] L. Bahl, J. Cocke, F. Jelinek, and J. Raviv, "Optimal decoding of linear

codes for minimizing symbol error rate," *IEEE Trans. Inform. Theory*, vol. IT-20, pp. 284–287, Mar. 1974.

[26] X. Li and J. A. Ritcey, "Bit-interleaved coded modulation with iterative decoding—Approaching Turbo-TCM performance without code concatenation," in *Proc. CISS'98*, Mar. 1998.

[27] J. Hagenauer and P. Hoeher, "A Viterbi algorithm with soft-decision outputs and its applications," in *Proc. IEEE GLOBECOM'89*, Nov. 1989, pp. 1680–1688.

[28] S. Benedetto, D. Divsalar, G. Montorsi, and F. Pollara, "Parallel concatenated trellis coded modulation," in *Proc. IEEE ICC'96*, June 1996, pp. 974–978.

[29] J. B. Cain and D. N. McGregor, "A recommended error control architecture for ATM networks with wireless links," *IEEE J. Select. Areas Commun.*, vol. SAC-15, pp. 16–27, Jan. 1997.

James A. Ritcey (S'74–M'83) received the B.S.E. degree from Duke University in 1976, the M.S.E.E. degree from Syracuse University in 1980, and the Ph.D. degree in electrical engineering (communication theory and systems) from the University of California, San Diego (UCSD), in 1985.

Since 1985, he has been with the Department of Electrical Engineering, University of Washington, where he now holds the rank of Professor. From 1981 to 1985, he was a Graduate Research Assistant at the Department of Electrical Engineering and Computer Sciences at UCSD. From 1976 to 1981, he was with the General Electric Company, and graduated from GE's Advanced Course in Engineering. His research interests include communications and statistical signal processing for radar, sonar, and biomedicine.

Dr. Ritcey served as the General Chair of the 1995 International Conference on Communications, Seattle, WA. He has also served as Technical Program Chair of the 1992 Asilomar Conference and General Chair of the 1994 Asilomar Conference on Signals, Systems, and Computers.

Xiaodong Li (M'97) received the B.S. degree from Tsinghua University, Beijing, China, in 1990, the M.S. degree from Shanghai Jiao Tong University, Shanghai, China, in 1992, and the Ph.D. degree from the University of Washington, Seattle, in 1998, all in electrical engineering.

From 1993 to 1998, he was a Research Assistant at the Department of Electrical Engineering, University of Washington. In 1996, he worked as a summer intern at the Wireless Systems Research Department, AT&T Laboratories—Research. Since 1998, he has been with the Wireless Technology Research Department, Bell Laboratories, Lucent Technologies, Holmdel, NJ. His general research interests include wireless data communications, networking, and video compression.